Since the downstream conditions have been altered, the shock will travel downstream with increasing velocity. Thus, an average shock velocity must be found from the velocities calculated at various distances along the nozzle. If the velocity of the starting shock at station z is V, then mass continuity across the shock gives

$$V=(\rho_* a_* A_*/A_z-\rho_z w_z)/(\rho_x-\rho_z) \tag{8}$$

Neglecting any change in stagnation conditions caused by the flow combination, the Mach number M_z downstream of the moving shock can be found from

$$w_z=(kp_{oy}/\rho_{oy})^{1/2}(1+M_z^2(k-1)/2)^{-1/2}M_z \tag{9}$$

and hence ρ_z can be found.

Mass continuity between the reservoir and the nozzle throat gives

$$\rho_* a_* A_* = w_t A_t (p_t)^{1/k} \tag{10}$$

and hence V can be found. If the average value of the velocity in traveling to the nozzle exit is V_2 then

$$t_2=L_2/V_2 \tag{11}$$

where L_2 is the length of the nozzle from throat to exit.

For the shock traveling through the test section, the conditions upstream of it are the given constant test section conditions, while the downstream conditions vary. Using an approach similar to the above, we find the shock velocity V at any point. In this case the area coefficient E in Eq. (7) is always unity. Mass continuity across the shock gives

$$V=(\rho_n w_n-\rho_z w_z)/(\rho_n-\rho_z) \tag{12}$$

Since w_n can be found from the given test section Mach number M_n then V can be calculated. If V_3 is the average shock velocity in the test section then

$$t_3=L_3/V_3 \tag{13}$$

where L_3 is the length of the test section.

Results and Comparison with Experiment

Schlieren observations were taken of the starting processes of the 4 nozzles of the Leeds University Supersonic Ludwieg Tube. The measured times of each starting phase are compared with the estimated times in Table 1. (There is no measured value of t_3 for the $M_n=4$ nozzle, since complete starting did not occur.) Furthermore, the previous theory has been applied to the MSFC high Reynolds number axisymmetric tunnel[5] with nitrogen at Mach 1.7 and 3.5

At Mach 2 and above the prediction of the starting times is accurate, even though the unsteady starting flow had a pronounced two-dimensional nature[2] while exhibiting such real gas effects as separation. In the transonic region agreement is poor, and it may be advantageous to revert to the method of characteristics[3] in this region, since the two-dimensional effects are not severe. Improved accuracy is unlikely with Falk's method[1] because the prediction of t_2 using the zero length nozzle analysis is very sensitive to the choice of conditions in the variable entropy region, downstream of the starting shock (e.g., for Falk's $M=3$ nozzle, a 1% change in the nondimensional sound speed at the edge of the variable entropy region causes approximately a 20% change in t_2). This virtually precludes the use of Falk's method, especially at the higher Mach numbers where the nozzle starting time t_2 is dominant.

Table 1 Measured (estimated) starting times in msec

M_n	t_1	t_2	t_3	t
1.4	4.3(3.1)	3.9(1.0)	4.0(1.0)	12.2(5.1)
2.0	3.1(2.6)	6.0(4.8)	4.4(1.9)	13.4(9.3)
3.0	2.9(2.3)	9.1(9.1)	3.0(2.2)	15.0(13.6)
4.0	2.9(2.2)	11.7(14.5)	(2.9)	(19.6)
1.7	(2.1)	(3.2)	(3.0)	21.0(8.3)
3.5	(2.6)	(20.6)	(4.4)	25.0(27.6)

The errors involved in the estimations of t are difficult to assess. The theoretical model is not truly representative of the physical situation, but the method does have the advantages that the complex flow regimes that actually occur during starting are not relevant to this analysis. Care must be taken in the numerical solution of the shock velocity very near the throat. This is because the equations are ill-conditioned and round-off errors become important near this region.

Conclusions

It had been shown previously that a more complicated analysis did not produce a reliable estimate of the nozzle starting times at the higher supersonic Mach numbers. The simpler one-dimensional method of this investigation incorporating a semiempirical equation is useful for predicting the starting times with reasonable accuracy, especially at the higher Mach numbers. These estimates are, in general, only to be used as a fairly rough guide to the expected starting times.

References

[1] Falk, T. J., "A Tube Wind Tunnel for High Reynolds Number Supersonic Testing," Rept. ARL 68-0031, Feb. 1968, Cornell Aeronautical Lab., Ithaca, N.Y.

[2] Barbour, N. McL., "An Investigation of the Mach Number Range and Performance of Two Intermittent High Speed Wind Tunnels," Ph.D. dissertation 1974, Dept. of Mechanical Engineering, University of Leeds, U. K.

[3] Warmbrod, J. D. and Struck, H. G., "Application of the Characteristic Method in Calculating the Time-Dependent, One-Dimensional Compressible Flow in a Tube Wind Tunnel," NASA TM X-53769, Aug. 1968.

[4] Davis, J. W., "A High Reynolds Number Wind Tunnel and its Operating Concept," *Journal of Spacecraft*, Vol. 5, Oct. 1968, pp. 1225-1227.

[5] Davis, J. W. and Gwin, H. S., "Feasibility Studies of a Short Duration High Reynolds Number Tube Wind Tunnel," NASA TM X-53571, Jan. 1968.

Impulse Loading of Finite Cylindrical Shells

M. J. Forrestal,* W. K. Tucker,† and W. A. Von Riesemann‡

Sandia Laboratories, Albuquerque, N. Mex.

SIMULATION of impulse loads produced by radiation induced material blowoff has recently received the attention of several investigators. The loading of rings with a cosine distributed impulse over half the ring circumference has been accomplished with explosives,[1,2] magnetically driven flyer plates,[3] and magnetic pressure pulses.[4] This Note describes a method of loading finite length cylindrical shells

Received February 10, 1975; revision received April 25, 1975. This work was supported by the U.S. Energy Research and Development Administration. The authors thank R. J. Goode and H. S. Tessler for performing the experiments.

Index category: Structural Dynamic Analysis.

*Division Supervisor, Shock Simulation Department. Associate Fellow AIAA.

†Staff Member, Shock Simulation Department.

‡Staff Member, Engineering Analysis Department.

with magnetically propelled flyer plates. The experimental arrangement is described, and application of the loading technique is demonstrated with an experiment on the elastic response of a circular cylindrical shell with free ends. In particular, excellent agreement is found between measured and predicted strains.

Experiments

A sketch of the experimental arrangement is shown in Fig. 1. The setup consists of a capacitor bank, a switch, and the flyer plate-load coil transmission line. When the switch is closed, a magnetic pressure is generated in the insulated region between the flyer plate and the load coil. The magnetic pressure accelerates the flyer plate to a cos θ velocity distribution and the impact of the flyer imparts a short-duration pressure pulse to the shell. As discussed in Refs. 3 and 4, magnetic pressure is proportional to the square of current per unit width normal to current flow. The cos θ velocity distribution of the flyer plate is achieved by varying the thickness of Mylar dielectric, which insulates the flyer plate and load coil. Briefly, current density is greater where the separation distance between conductors is smaller. The design for the θ-distribution of Mylar is complex and it is achieved with the aid of the computer program described in Ref. 5. For these experiments, the θ-distribution of Mylar is accomplished by gluing together 10 thin strips of Mylar between two sheets which extend over $|\theta| < 80°$. The dielectric spacing is reasonably smooth over $|\theta| < 80°$, and varies from 0.008 in. at $\theta = 0°$ to 0.038 in. at $\theta = 80°$.

For this structural impact experiment, the flyer plate consists of 0.030-in. polyethylene with specific gravity 0.92 and 0.006-in. 1100-0 aluminum.§ There is an air layer between the flyer and the cylindrical shell, which is compressed as the flyer approaches the cylinder. The air layer acts as a spring and eventually causes the flyer to rebound back towards the load coil; consequently, the impulse delivered to the cylinder is greater than the incoming flyer momentum. Flyer velocity and arrival time are measured with an array of six pin switch pairs mounted on the shell at $\theta = 0°$, 1.0 in. either side of center; and at $\theta = \pm 30°$ and $\theta = \pm 60°$ in the center plane. Cylinder motion is measured with a framing camera.

Cylindrical shells were machined from 2014-T651 aluminum round stock to an outer diameter 6.865 in. and thickness 0.166 in. As shown in Fig. 1, the 6.00-in. long shell is suspended by thin glass rods. The flyer-to-shell gaps are 0.070 in. at $\theta = 0°$ and 0.022 in. at $\theta = 80°$.

Results and Comparisons with Predictions

Two sets of experiments were conducted. The first set of experiments emphasized diagnostics of the setup; namely, flyer plate velocity distribution and impulse delivered to the cylinder. The θ-distribution of Mylar spacing between load coil and flyer determines the incoming flyer velocity as a function of θ. After a few preliminary experiments and code runs,[5] the Mylar spacing was adjusted to bring the measured velocity distribution within 10% of theoretical. Once the θ-spacing of Mylar was acceptable, two experiments were conducted in which the peak impulse intensities delivered to the cylinder were determined from framing camera data to be 179 and 178 Pa·s.¶ The ratio of cylinder impulse to incoming flyer momentum for both experiments was 1.53.

For the second set of experiments, circumferential strains were measured with two Micro-Measurements EA-07-125-AC-350 strain gages mounted to the inner and outer surfaces in the cylinder center plane at $\theta = 180°$. Oscillograms of the circumferential membrane strain $\epsilon_m = \frac{1}{2}(\epsilon_i + \epsilon_o)$ and bending strain $\epsilon_b = \frac{1}{2}(\epsilon_i - \epsilon_o)$, where ϵ_i and ϵ_o are the strains on the inner and outer surfaces, are shown in Fig. 2. Predictions of the strain-time histories were obtained from the finite element computer program DYNAPLAS[6] for the peak impulse intensity 167 Pa·s. DYNAPLAS uses a shell of revolution

§Current is carried by the aluminum; the polyethylene is on the impact side.

¶1 Pa·s = 0.10 dyne-sec/cm^2 = 1.45×10^{-6} psi-sec.

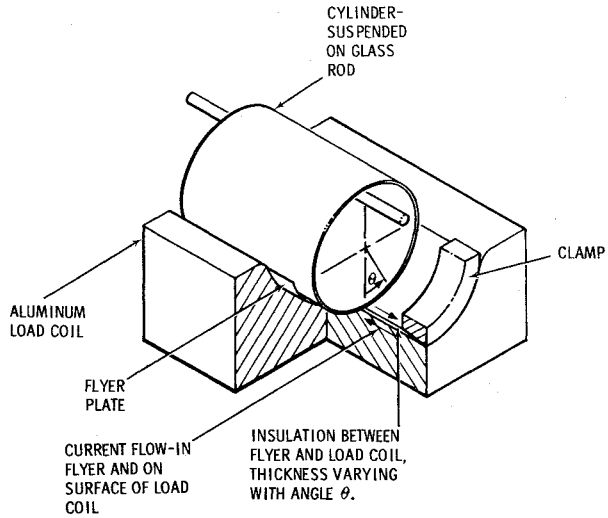

Fig. 1 Experimental arrangement.

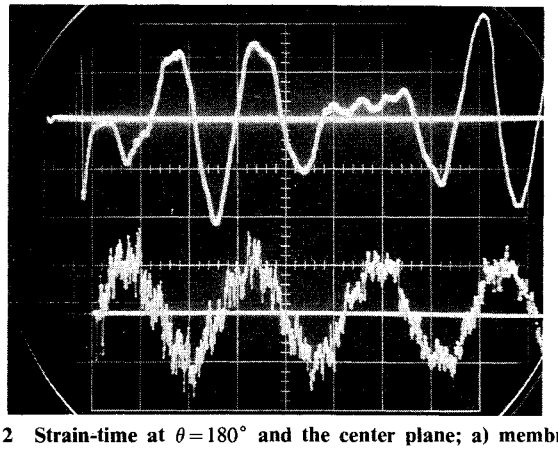

Fig. 2 Strain-time at $\theta = 180°$ and the center plane; a) membrane strain 1000 $\mu\epsilon$/div, 50 μs/div; b) bending strain 1000 $\mu\epsilon$/div, 1 ms/div.

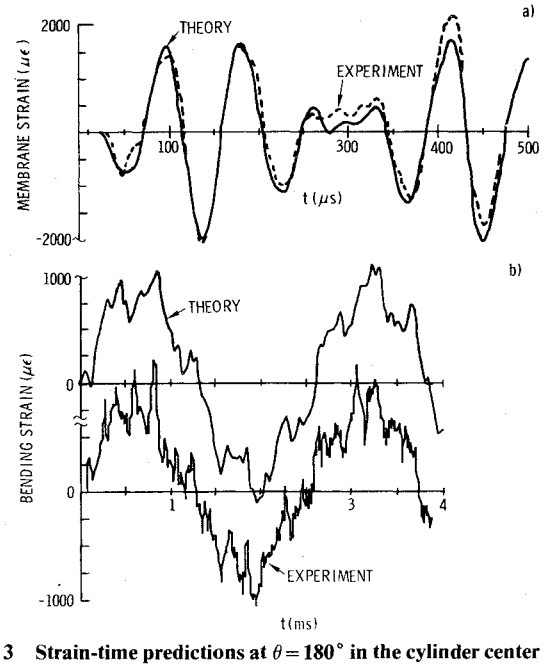

Fig. 3 Strain-time predictions at $\theta = 180°$ in the cylinder center plane; a) membrane strain, b) bending strain.

element and a Fourier expansion in the circumferential direction. The predictions sum seven modes (n = 0 to n = 6) and comparisons of the measured and predicted strains are shown in Figs. 3a and b. Bending strain response is dominated by the fundamental bending mode (n = 2) and has lower amplitude, higher frequency modes superimposed.

As indicated in Fig. 3, excellent agreement is found between measured and predicted strains for this experimental setup. These simple structural experiments are used in our laboratory to select reasonable flyer plate designs and flyer-to-shell air gaps before testing full-scale systems.

References

[1]Benham, R. A. and Mathews, F. H., "X-Ray Simulation with Light-Initiated Explosive," *The Shock and Vibration Bulletin,* Bulletin 45, Oct. 1974, pp. 21-22

[2]Lindberg, H. E. and Kennedy, T. C., "Dynamic Plastic Pulse Buckling in Beyond Strain-Rate Reversal," *Journal of Applied Mechanics*, Vol. 42, No. 2, June 1975, pp. 411-416.

[3]Bealing, R., "Impulse Loading of Circular Rings," *Experimental Mechanics, Proceedings of the 11th Annual Symposium,* University of New Mexico, 1971, pp. 15-26.

[4]Forrestal, M. J. and Overmier, D. K., "An Experiment on an Impulse Loaded Elastic Ring." *AIAA Journal*, Vol. 12, May 1974, pp. 722-724.

[5]Tucker, W.K., "Two Digital Computer Programs for Flyer Plate-Capacitor Bank Analysis," SC-DR-70-122, April 1970, Sandia Laboratories, Albuquerque, N. Mex.

[6]Stricklin, J. A., Haisler, W. E., and Von Riesemann, W. A., "Large Deflection Elastic-Plastic Dynamic Response of Stiffened Shells of Revolution," *Journal of Pressure Vessel Technology,* Vol. 96, Series J, May 1974, pp 87-95.

Expansion Tube With Nozzle Plate: Theory and Experiment

F. H. Oertel Jr.,* N. Gerber,*

and

J. M. Bartos†

U. S. Army Ballistic Research Laboratories, Aberdeen Proving Ground, Md.

Introduction

THE expansion tube uses unsteady expansion to generate high-enthalpy high-velocity flows of test gases initially isolated in the driven section by the first and second diaphragms (Fig. 1)—on one side against the high-pressure driver gases and on the other against the evacuated expansion section. The BRL expansion tube has been used to make measurements in nonequilibrium shock layers as selected gases flowed past axisymmetric bodies. For those experiments, it was desirable to have a freestream flow uniform in density and velocity with low dissociation and low impurity level.

An earlier paper[1] reported extensive investigations of test flow characteristics in our original expansion tube (using simply-supported mylar second diaphragms) and preliminary results in the modified tube (using scribed metal second diaphragms placed adjacent to a perforated plate, called a nozzle plate.[2]) Test flows in the original tube were found to be quite uniform for the most part—density fluctuations were typically less than ±15%.[3] However, it appeared that with the nozzle plate the flow could be made more uniform (and more contamination-free) by forcing the diaphragm to petal open along the scribes into the holes of the nozzle plate; and model and instrumentation damage could be reduced, since the nozzle plate blocks first diaphragm particles.

The purpose of this paper is to present results of computations of test flow properties which supplement limited preliminary data[1,2] and, for the first time, to evaluate the computation model by experimental results. In our experiments, we use a new nozzle plate design suggested by the results of Refs. 1 and 2.

Computations

We adopted the operation cycle for the modified expansion tube shown in the x-t diagram of Fig. 1. For the computations we assumed that: 1) diaphragms open ideally; 2) expansion waves are isentropic centered rarefactions; 3) one-dimensional conservation equations for an inviscid, non-conducting, diatomic gas in vibrational and chemical equilibrium are valid; 4) steady quasi-one-dimensional flow in a single nozzle with an effective area ratio, A/A^*, is applicable (A = cross-sectional area of expansion tube, A^* = sum of nozzle throat areas); and 5) the first shock is fully reflected from the second diaphragm before the diaphragm opens.

The governing equations are given in Ref. 4, and the numerical-graphical procedure used to solve them is outlined there. Flow properties in each section of the expansion tube were computed for the following range of parameters: 1) first shock Mach number, M_{s_1}: 3-9; 2) initial pressure in the driven section, P_1: $2.76\times10^4 N/m^2$-$8.28\times10^4 N/m^2$; 3) initial pressure in the expansion section, P_{10}: $6.66 N/m^2 - 26.7 N/m^2$; 4) effective nozzle area ratio, A/A^*: 2 (new nozzle plate)[5] and 4 (first nozzle plate)[2]; 5) initial temperatures in driven and expansion sections, T_1 and T_{10}: 300°K.

From an operational standpoint, the most important properties of the test gas are the density ρ_5 and the velocity u_5 in the test section. They are plotted in Fig. 2 for the new nozzle plate ($A/A^* = 2$). Each symbol gives the result of a computation for real air and a discrete set of initial parameters. The degree to which initial parameters affect properties in the test section is summarized in Table 1.

Experimental Measurements and Techniques

The experimental measurements and techniques used here have been described in detail.[1,3] Detailed descriptions of the

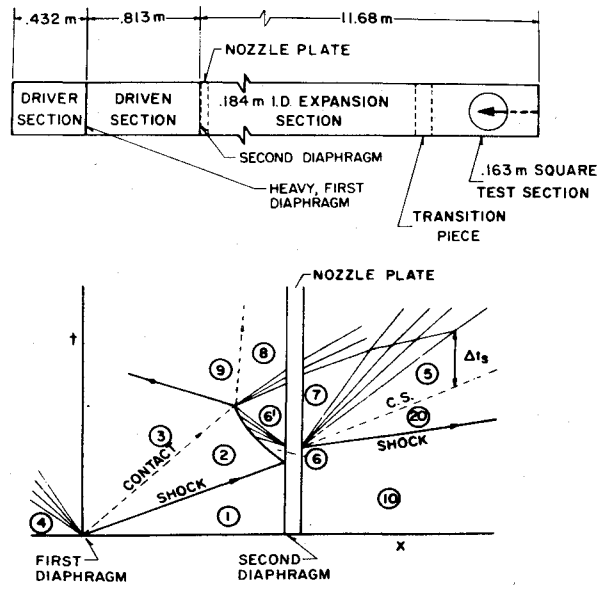

Fig. 1 Sketch of modified expansion tube and $x-t$ diagram showing full reflection of first shock.

Received February 14, 1975.

Index categories: Supersonic and Hypersonic Flow; Research Facilities and Instrumentation.

*Aerospace Research Engineer. Member AIAA.

†Mathematician.